A study on the modulation of the electrical transport by mechanical straining of individual titanium dioxide nanotube

A. Asthana,[1,a)] T. Shokuhfar,[1,2] Q. Gao,[1] P. Heiden,[3] C. Friedrich,[1,2] and R. S. Yassar[1,a)]
[1]*Department of Mechanical Engineering-Engineering Mechanics, Michigan Technological University, Houghton, Michigan 49931, USA*
[2]*Multi-Scale Technologies Institute, Michigan Technological University, Houghton, Michigan 49931, USA*
[3]*Departmentof Chemistry, Michigan Technological University, Houghton, Michigan 49931, USA*

(Received 17 March 2010; accepted 16 June 2010; published online 17 August 2010)

We report here, the deformation driven modulation of the electrical transport properties of an individual TiO_2 nanotube via *in situ* transmission electron microscopy (TEM) using a scanning tunneling microscopy system. The current-voltage characteristics of each individual TiO_2 nanotube revealed that under bending deformation within the elastic limit, the electrical conductivity of a TiO_2 nanotube can be enhanced. High resolution TEM and electron diffraction pattern reveal that TiO_2 nanotubes have tetragonal structure (a=0.378 nm, c=0.9513 nm, $I4_1/amd$). Analysis based on a metal-semiconductor-metal model suggests that in-shell, surface defect-driven conduction modes and electron–phonon coupling effect are responsible for the modulated semiconducting behaviors. © *2010 American Institute of Physics*. [doi:10.1063/1.3466663]

The semiconducting behavior of 1D titania (TiO_2) in various morphologies (tubes, wires, fibers, and rods) and large surface area have drawn considerable attention for potential applications in solar cells,[1] gas sensors, lithium ion batteries and biomedical systems.[2,3] However, the widespread technological use of titania is impaired by its wide band gap (3.2 eV), which requires ultraviolet (UV) irradiation for photocatalytic activation.[2,3] Traditionally, doping of the titania has been the approach taken for its band gap engineering.[4]

Here, we propose an alternate way to enhance the electrical conductivity of TiO_2 nanotube using mechanical straining. A recent theoretical work on boron nitride nanotubes (BNNTs) under flattening deformation[5] has predicted the unique possibility of band gap tuning in a 2–5 eV range. This theoretical prediction on BNNTs has been experimentally verified by Bai *et al.*[6] by a series of *in situ* scanning tunneling microscopy (STM) experiments in a transmission electron microscope (TEM).

The crystal structure of the TiO_2 phase affects the photoelectrical current in solar cells and anatase based solar cells are expected to have the highest conversion efficiency. This effect has been attributed to the higher Fermi level in anatase in comparison to that of rutile by about 0.1 eV.[7]

In view of this, we report here, the effect of mechanical deformation on an electrical response of an individual anatase TiO_2 nanotubes. There are few reports on the electrical transport properties of an array of TiO_2 nanotubes and thin films.[8,9]

All the electrical measurements were carried out on a single tilt STM-TEM holder in a JEM 4000FX TEM system that operated at 200 keV. In the present investigations, TiO_2 nanotube samples were synthesized by anodization of TiO_2 foils for 8 h at 60 V. The synthesis process is almost similar to that of reported by Schmuki and co-workers[10] and Djenizian and co-workers.[11]

The structural investigations of TiO_2 nanotube samples were carried out during the *in situ* TEM experiment. Figure 1(a) shows an overall view of the anatase titania nanotube, depicting a number of tubular nanostructures with uniform size distribution. The tubes are hollow and open ended with an average inner and outer diameter of approximately 25 and 70 nm and the lengths range to several hundreds of nanometers. The corresponding diffraction pattern is shown in the inset [Fig. 1(a)], depicting the anatase titania (a=0.378 nm, c=0.9513 nm, $I4_1/amd$). The HRTEM image [Fig. 1(b)] taken from a single nanotube [inset of Fig. 1(b)] shows that the nanotubes are well crystalline. The lattice fringe spacing of the walls of the nanotubes is estimated to be ~0.353 nm, corresponding to the interplanar distance of the (101) plane in the anatase phase.

To ensure good electrical contact between the tip and the nanotube for *in situ* electrical measurement, an individual TiO_2 nanotube was attached to the electromechanically etched gold tip by tungsten deposition using the focused ion beam (FIB) technique. The different steps of the sample preparation are shown in Figs. 2(a)–2(c). In short, a nanotube was picked up using the FIB probe [Figs. 2(a) and 2(b)] and attached on the gold tip [Fig. 2(c)] by the tungsten deposition. The gold tip with TiO_2 nanotube was then transferred to the STM-TEM specimen holder and approached to its opposite conducting STM tip by the piezomanipulator. A schematic diagram of the experimental setup is shown in Fig. 2(d).

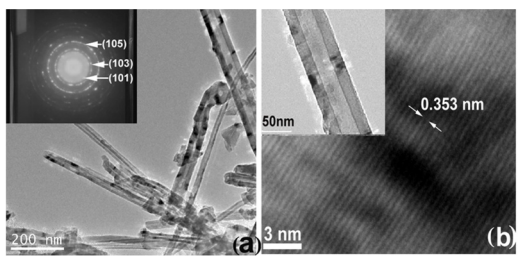

FIG. 1. (Color online) (a) An overall view of the anatase titania nanotube and the corresponding diffraction pattern (inset) and (b) the high resolution lattice image from a single anatase nanotube (inset).

[a)]Authors to whom correspondence should be addressed. Electronic addresses: aasthana@mtu.edu and reza@mtu.edu.

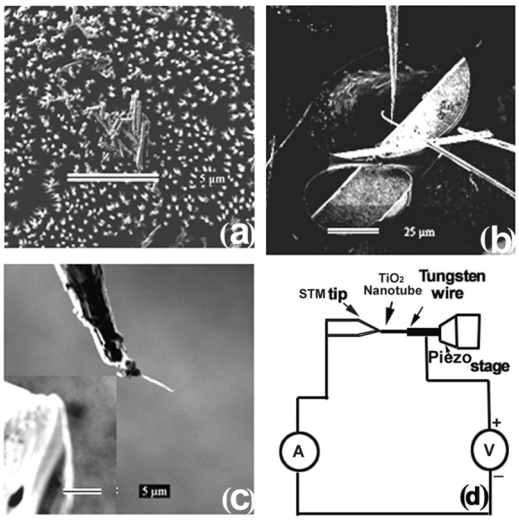

FIG. 2. Images from the FIB system show (a) the as grown TiO_2 nanotube sample; (b) FIB probe attached with a single nanotube, dispersed on the Cu mesh; (c) the FIB probe with a nanotube approaching the tip of the tungsten wire and; (d) schematic of the experimental setup for current–voltage measurement.

Figures 3(a)–3(e) display the sequential images of a typical TiO_2 nanotube approaching the STM tip and undergoing a gradual increase in its bending curvature by incremental movement of the piezodriven gold tip toward the STM tip. A series of measured *I-V* curves at various stages of bending deformation are, respectively, shown in Fig. 3(f). The TiO_2 nanotube in contact with the STM tip [Fig. 3(c)] shows a semiconducting behavior where electrical currents up to 10 nA can be detected under bias voltages up to 25 V [curve "c" in Fig. 3(f) corresponding to Fig. 3(c)]. The similar semiconducting electrical transport behavior was also observed for an array of anatase TiO_2 nanotube and thin films.[8,9] This is due

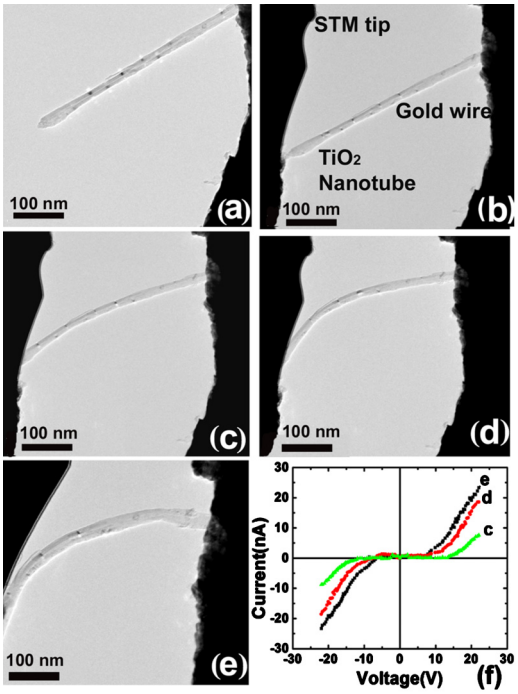

FIG. 3. (Color online) The bight field image of the TiO_2 nanotube (a) approaching the STM tip; (b) in contact with the STM tip; [(c)–(e)] undergoing a gradual increase in its bending curvature; (f) a series of the representable *I-V* curves measured during the deformation of the TiO_2 nanotubes.

to the intrinsic semiconducting behavior of the TiO_2 nanotube under the applied voltage. As we deform the nanotube, attached with the tungsten wire against the STM tip, current upto 18 nA can be observed (curve "d") for the deformed state corresponding to Fig. 3(d). With the increase in deformation [Fig. 3(e)], the current is dramatically increased to 25 nA with start off voltage of 7.5 V bias as is evident from curve "e" [Fig. 3(f)]. Figure 3(e) displays the TiO_2 nanotube in the highest deformed state under the present study, making a large bending curvature and corresponds to the state of the *I-V* curve "e." In a large bias regime, the *I-V* curve can be differentiated to obtain a resistance *R* of the nanowire ($R \sim dV/dI$,). We found that for this deformed state, the resistance of the nanotube was decreased to 0.34 GΩ from ~0.86 GΩ in the state corresponding to Fig. 3(c).

The nonlinear and symmetrical *I-V* characteristics of these deformed states suggests a semiconducting behavior. Thus our measurement system can be regarded as a metal-semiconductor-metal (M-S-M) circuit.[12] The related semiconducting parameters can be retrieved from the experimental *I-V* data in the bias regime >5 V, by the following relation[6,13]

$$\ln I = \ln S + V\left(\frac{q}{k_B T} - \frac{1}{E_0}\right) + \ln J_s. \quad (1)$$

Here *S* is the contact area associated with a bias, J_s is the saturation current density, and *V* is the slowly varying function of the applied bias. The $\ln I$ versus *V* plot gives an approximately straight line with a slope of $(q/k_B T) - 1/E_0$, and an intercept of $\ln S$. The representative $(\ln I)$-*V* curves are depicted in Figs. 4(a) and 4(b) corresponding to curve d and curve e in Fig. 3(f), respectively. Figure 4(c) shows the linear fits of curve d and e extrapolated to the $\ln I$ axis, showing nearly identical values of intercept. This means, $\ln S$ and the contact area (*S*) is nearly identical for both of these stressed states. In the expression of $\ln I$, $E_0 = E_{00} \coth(E_{00}/k_B T)$, where $E_{00} = (\hbar q/2)[n/(m^* \varepsilon)]^{1/2}$. Here, *q* is the elemental charge, k_B is the Boltzmann constant, m^* is an effective electron mass of TiO_2 nanotube, and ε is the permittivity. We have estimated the specific sizes of the nanotube from the bright field TEM image and thus the resistivity, ρ is obtained. The electron mobility, μ, is then calculated by using the relationship $\mu = 1/(nq\rho)$. For anatase TiO_2 thin films, the dielectric constant, *k* is close to the value between 25–30, therefore, the value of permittivity, ε is taken as $\varepsilon = 26\varepsilon_0$,[14] ε_0 is the dielectric constant of a vacuum and $m^* = 1.26 m_0$.[15] Based on this procedure, the resistance, resistivity, carrier concentration and carrier mobility were extracted as summarized in Table I. These values are in conformity with those obtained for the anatase TiO_2 thin films and single crystal of TiO_2.[16–19] The *I-V* measurement with bending deformation were repeated for several times to ensure the reproducibility of the data.

Under the present study, it was interesting to note that the electrical conductivity of TiO_2 nanotubes can be modulated by the mechanical deformation. Such phenomena can be related to the strain engineering of the electronic band gap structure in nanotubes.[20,21] It can be said that in the present study, when the anatase TiO_2 nanotubes are brought into deformed state, in-shell defects are produced at the walls of the nanotube. The possible defects can be voids, vacancies, and antisite atoms, which modify the band structure.[22] The carri-

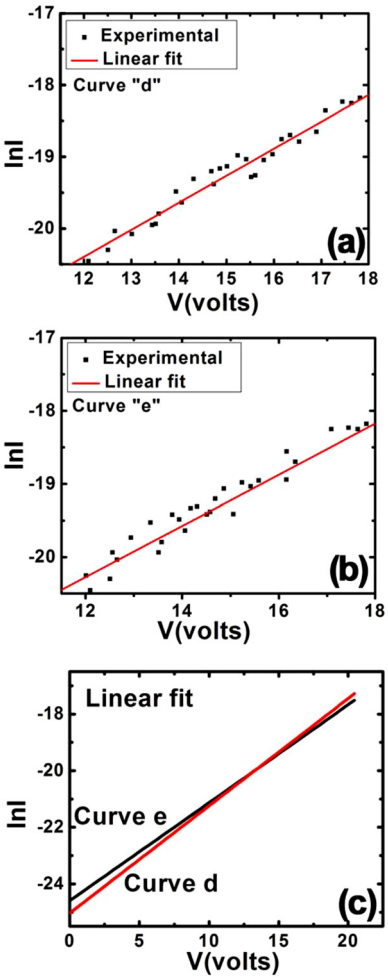

FIG. 4. (Color online) The ln *I-V* curves corresponding to (a) curve *d* and (b) curve *e* in Fig. 3(f), respectively. (c) The linear fits of the curves in [(a) and (b)].

ers of current, i.e., electrons in this case (as TiO_2 is considered as *n* type semiconductor) are scattered strongly by the disordered structure, so that the mean free path of electrons may sometime be the order of the scale of the disorder. The pinning of the Fermi level is known to arise from the presence of defects,[23] such as dangling bonds and other misfits in the structure, which produce localized state in the gap. Hence, the TiO_2 nanotube in a higher deformed state will produce more defects, so a large number of electrons are scattered by the formation of a large number of defects. The production of defects will also help in the pinning of the Fermi level, which will produce a localized state in the gap and hence help in the transport of the electrical current through the TiO_2 nanotube.

TABLE I. Electrical parameters of TiO_2 nanotube.

Parameters	Curve c	Curve d	Curve e
Resistance (GΩ)	0.86	0.66	0.34
Resistivity (Ω cm)	43.5	36.4	16.36
E_0 (meV)	23.98	24.9	27.0
Carrier concentration (cm^{-3})	0.78×10^{17}	1.58×10^{17}	3.5×10^{17}
Mobility ($cm^2/V\,s$)	2.05	1.08	1.05

Another possibility for the increase in current by deformation can be due to the presence of dangling bonds at the surface of the TiO_2 nanotube. These defects can have a dominant role in modulating its electrical conductivity.[24,25] Surface defects can produce surface states within the band gap making the TiO_2 nanotube behaves like a weakly conductive metal. This allows the flow of conduction electrons near the surface region of the TiO_2 nanotube as also reported by Lin *et al.*[26]

In conclusion, it was shown that the electrical transport properties of the TiO_2 nanotube could be enhanced by inducing deformation into the nanotube using an *in situ* STM-TEM stage. The semiconducting parameters were retrieved from the experimental *I-V* curves using the M-S-M model. Here, it can be emphasized that, considering the deformation driven electrical property modulation of the TiO_2 nanotube as observed in the present investigations, the TiO_2 nanotube holds a promising future and perspective candidate for constructing nanoscale electronic and optoelectronic devices and more importantly for its usage in solar cell applications.

RSY would like to appreciate the funding support through the NSF-DMR Grant No. 0820884 and NSF-CMMI Grant No. 0926819.

[1]M. Adachi, Y. Murata, I. Okada, and S. Yoshikawa, J. Electrochem. Soc. **150**, G488 (2003).
[2]O. K. Varghese, D. Gong, M. Paulose, K. G. Paulose, and C. A. Grimes, Sens. Actuators B **93**, 338 (2003).
[3]G. Armstrong, A. R. Armstrong, P. G. Bruce, P. Reale, and B. Scrosati, Adv. Mater. (Weinheim, Ger.) **18**, 2597 (2006).
[4]T. Umebayashi, T. Yamaki, H. Itoh, and K. Asai, J. Phys. Chem. Solids **2**, 5320 (2002).
[5]Y. H. Kim, K. J. Chang, and S. G. Louie, Phys. Rev. B **63**, 205408 (2001).
[6]X. Bai, D. Goldberg, Y. Bando, C. Zhi, C. Tang, M. Mitome, and K. Kurashima, Nano Lett. **7**, 632 (2007).
[7]H. P. Maruska and A. K. Gosh, Sol. Energy **20**, 443 (1978).
[8]Y. K. Lai, L. Sun, C. Chen, C. G. Nie, J. Zuo, and C. J. Lin, Appl. Surf. Sci. **252**, 1101 (2005).
[9]M. Villafuerte, G. Juarez, S. P. de Heluani, and D. Comedi, Physica B **398**, 321 (2007).
[10]J. M. Macak, H. Tsuchiya, S. Berger, S. Bauer, S. Fujimoto, and P. Schmuki, Chem. Phys. Lett. **428**, 421 (2006).
[11]G. F. Ortiz, I. Hanzu, P. Knauth, P. Lavela, J. L. Tirado, and T. Djenizian, Electrochim. Acta **54**, 4262 (2009).
[12]F. A. Padovani and R. Stratton, Solid-State Electron. **9**, 695 (1966).
[13]Z. Y. Zhang, C. H. Jin, X. L. Liang, Q. Chen, and L.-M. Peng, Appl. Phys. Lett. **88**, 073102 (2006).
[14]M. Stamate, G. Lazar, and I. Lazar, Rom. J. Phys. **53**, 217 (2008).
[15]H. Tang, K. Prasad, R. Sanjines, P. E. Schmidt, and F. Levy, J. Appl. Phys. **75**, 2042 (1994).
[16]E. Hendry, F. Wang, J. Shan, T. F. Heinz, and M. Bonn, Phys. Rev. B **69**, 081101 (2004).
[17]E. Yagi, R. R. Hasiguti, and M. Aono, Phys. Rev. B **54**, 7945 (1996).
[18]G. A. Acket and J. Volger, Physica (Amsterdam) **30**, 1667 (1964).
[19]V. N. Bogomolov and V. P. Zhuze, Sov. Phys. Solid State **5**, 2404 (1964).
[20]H. Y. Peng, M. D. McCluskey, Y. M. Gupta, M. A. Kneissl, and N. M. Johnson, Phys. Rev. B **71**, 115207 (2005).
[21]K. Nishidate and M. Hasegawa, Phys. Rev. B **78**, 195403 (2008).
[22]S. D. Mahanti, K. Hoang, and S. Ahmad, Physica B **401**, 291 (2007).
[23]J. Robertson, O. Sharia, and A. A. Demkov, Appl. Phys. Lett. **91**, 132912 (2007).
[24]M. Huang, P. Rugheimer, M. G. Lagally, and F. Liu, Phys. Rev. B **72**, 085450 (2005).
[25]M. S. Arnold, P. Avouris, Z. W. Pan, and Z. L. Wang, J. Phys. Chem. B **107**, 659 (2003).
[26]X. Lin, X. B. He, T. Z. Yang, W. Gao, D. X. Shi, H.-J. Gao, D. D. D. Ma, T. S. Lee, F. Liu, and X. C. Xie, Appl. Phys. Lett. **89**, 043103 (2006).